INTERNATIONAL JOURNAL FOR NUMERICAL METHODS IN FLUIDS, VOL. 13, 671–690 (1991)

FINITE DIFFERENCE REPRESENTATIONS OF NON-LINEAR WAVES

GEIR PEDERSEN

Department of Mechanics, University of Oslo, PO Box 1053, Blindern, N-0316 Oslo 3, Norway

SUMMARY

The work concerns cnoidal and solitary wave solutions of the Boussinesq equations in the context of finite difference methods. The existence of permanent wave-forms is discussed and approximate solutions are found for one particular discrete formulation by perturbation techniques. These techniques can be applied to most difference and regular element discretizations of equations describing weakly non-linear and dispersive waves. No proof of convergence of the perturbation expansions is established, but the appropriateness of the solutions is confirmed through comparison with the results of computer simulations. From the perturbation series it is found that the phase speed of solitons is useless for the evaluation of numerical methods and that asymmetries in the discrete equations may ruin the soliton solution. The availability of a discrete closed-form solution is especially important for discussions concerning the existence and accuracy of permanent wave-forms with oblique orientations relative to the grid.

KEY WORDS Non-linear waves Finite differences Boussinesq equations

1. INTRODUCTION

One of the most instructive ways of evaluating a numerical method is to investigate its capability of reproducing simple analytical solutions. Often this involves a large number of test runs on a computer with uncertainties concerning code errors, limitations on grid resolutions and the introduction of unwanted boundary conditions. However, in many cases 'manual' analysis of the methods may provide an attractive alternative. For wave problems the most important example is Fourier analysis which is applicable to linear equations with constant coefficients. Unfortunately, such analysis is seldom carried beyond the establishment of dispersion relations and simple stability criteria. Nevertheless, classical methods of analysis, traditionally applied to differential equations, often work equally well with discretized problems. Thus discrete solutions of closed form may occasionally be derived for problems involving coupling between modes, non-trivial boundary conditions or non-linearities. Such solutions are of great value both for evaluating numerical methods and for the validation of computer programmes. The solutions could be viewed as analytical solutions to discrete problems. However, we will avoid such terms and reserve the notation 'analytical' for the direct treatment of differential equations. In the present paper we will study numerical representations of some simple solutions of the non-linear Boussinesq equation.

For surface gravity waves in shallow water there are two important non-linear solutions of permanent form, namely the soliton and the periodic cnoidal wave. Both are important in the context of complex wave patterns as well as representative of non-linear waves in their own right. Particularly the soliton has received appreciable attention in the literature. The remarkable collision properties of these non-linear waves have been studied in a series of papers through the

0271–2091/91/160671–20$10.00

Received December 1989
Revised November 1990

last decades, some of which involve numerical integration. Also the propagation of solitons over shelves and their run-up on vertical or inclined planes have been extensively studied (see e.g. References 1–6). These works do not focus exclusively on the peculiar properties of the soliton solution itself, but also on features concerning non-linear waves in general. An example is the question of non-linear modifications to Green's law for amplification in shoaling water. In recent years the topic of non-linear ship wave patterns in shallow water has become popular. Particular attention has been paid to the upstream radiation of solitons that has been observed in the transcritical regime.[7–12,30] The non-linear shallow water theories also describe ocean waves in coastal regions and their impact on harbours, etc. These are the motivation for works such as References 13–16.

Even though soliton and cnoidal wave solutions are also widely used for the validation of numerical techniques, the problem of finding numerical counterparts to the analytical solutions has hardly been addressed. In the limit of very refined grid resolutions one would always expect to reproduce the solutions fairly well, at least for moderate time intervals. Still, many problems involving slow evolution, refraction, interaction, etc. of solitons will be very sensitive to even extremely slow numerical growth/damping or disintegration of the wave-forms. Besides, such cases generally require the discretization of large domains with corresponding limitations on the grid increments. As a consequence, the results of the computations may be confused or even dominated by spurious effects.

The succeeding sections will contain approximate closed-form solutions for solitary and cnoidal waves moving in a finite difference grid. The study of the latter wave type will be confined to the Stokes wave limit (small Ursell numbers). Cases of intermediate and large Ursell numbers can probably be treated analogously as for the soliton, but we believe that the addition of such an analysis will give but little new insight of the numerics. The work will be concentrated on a particular shallow water formulation and numerical techniques that have been used previously by the author. Nevertheless, the principles of the analysis will apply equally well to most finite difference and finite element discretizations on a regular mesh.

2. FORMULATION

The equations will be formulated in a co-ordinate system with the horizontal axes Ox^* and Oy^* in the undisturbed water level and the vertical axis Oz^* pointing upwards. The asterisks indicate dimensional quantities. The fluid is confined to $-h^* < z^* < \eta^*$ and the depth-averaged velocity and velocity potential are denoted by $\mathbf{v}^*$ and ϕ^* respectively. We introduce a characteristic depth h_0, a characteristic horizontal length l, amplitude αh_0 and dimensionless variables according to

$$\begin{aligned} &z^* = h_0 z, && x^* = lx, && y^* = ly, \\ &t^* = l(gh_0)^{-1/2} t, && \eta^* = \alpha h_0 \eta, && \\ &\phi^* = \alpha l (gh_0)^{1/2} \phi, && \mathbf{v}^* = \alpha (gh_0)^{1/2} \mathbf{v}, && \end{aligned} \tag{1}$$

where g is the acceleration of gravity. The x- and y-components of $\mathbf{v}$ will be referred to as u and v respectively. In various sections we will use different horizontal length scales l. Regarding the discussion of relative errors and dominant balances in the equations, the appropriate choice for l is a typical wavelength. This definition is used in Sections 2.1 and 2.2 and in the formulation of the perturbation expansions in the succeeding sections. To make comparisons easier within the paper as well as with other works, we also introduce a reference scaling based on using the depth as both horizontal and vertical length scale. This leads to the following definitions of $\hat{x}$, $\hat{y}$, $\hat{t}$ and $\hat{\eta}$:

$$\hat{x} = x^*/h_0, \qquad \hat{y} = y^*/h_0, \qquad \hat{t} = (gh_0)^{1/2} t^*/h_0, \qquad \hat{\eta} = \eta^*/h_0. \tag{2}$$

Scaling according to the above set of relations will be used for presenting the final results, both in expressions and figures, and for the description of computer simulations.

In the context of vertically integrated theories such as the shallow water theories the use of the phrases 'three-' and 'two-dimensional' may be ambiguous. We prefer to use the phrases in the physical sense, which means that a three-dimensional wave is one that involves motion in two horizontal directions in addition to vertical elevation. Thus the integrated equations describing a three-dimensional wave contain only two space variables.

2.1. *The Boussinesq equation*

For long waves in shallow water, weakly dispersive and non-linear theories can be established through expansions in the small parameters α and $\varepsilon \equiv h_0^2/l^2$, where l is a characteristic wavelength. The resulting equations may be cast into a variety of forms according to the choice of variables, extra assumptions, etc. In the subsequent sections we will mainly be concerned with one particular version of the Boussinesq equations. Other important shallow water equations are the KdV (Korteweg–deVries) equation, which describes unidirectional waves, and the KP (Kadomtsev–Petviashvili) equation, which is a weakly three-dimensional generalization of the KdV equation. Derivations and discussion of Boussinesq equations are given in many textbooks and articles. References 11 and 17–19 are of particular relevance to the present work.

In the case of constant depth the Boussinesq equations expressed in terms of the depth-averaged velocity potential read

$$\eta_t = -\nabla\cdot\{(1+\alpha\eta)\nabla\phi\} + O(\alpha\varepsilon), \tag{3}$$

$$\phi_t + \tfrac{1}{2}\alpha(\nabla\phi)^2 + \eta - \tfrac{1}{3}\varepsilon\nabla^2\phi_t = O(\varepsilon^2, \alpha\varepsilon). \tag{4}$$

In three dimensions this set is solved numerically in References 11 and 16. Recognizing $\nabla\phi$ as $\mathbf{v}$, the average horizontal velocity, the equations may be rewritten to give

$$\eta_t = -\nabla\cdot\{(1+\alpha\eta)\mathbf{v}\}, \tag{5}$$

$$\mathbf{v}_t + \tfrac{1}{2}\alpha\nabla(\mathbf{v}^2) = -\nabla\eta + \tfrac{1}{3}\varepsilon\nabla^2\mathbf{v}_t, \tag{6}$$

which is another formulation that is frequently used.

2.2. *The numerical procedure*

We will concentrate the study on the numerical techniques discussed and used in References 11, 15, 19 and 20. In the present paper we will only recapitulate the methods briefly, including some useful nomenclature.

The approximation to a quantity f at a grid point with co-ordinates $(\beta\Delta x, \gamma\Delta y, \kappa\Delta t)$, where Δx, Δy and Δt are the grid increments, is denoted by $f_{\beta,\gamma}^{(\kappa)}$. To improve the readability of the difference equations, we introduce the symmetric difference operator δ_x by

$$\delta_x f_{\beta,\gamma}^{(\kappa)} = \frac{1}{\Delta x}\left(f_{\beta+1/2,\gamma}^{(\kappa)} - f_{\beta-1/2,\gamma}^{(\kappa)}\right) \tag{7}$$

and the midpoint average operator $(\bar{\ }^{x})$ by

$$(\bar{f}^x)_{\beta,\gamma}^{(\kappa)} = \tfrac{1}{2}\left(f_{\beta-1/2,\gamma}^{(\kappa)} + f_{\beta+1/2,\gamma}^{(\kappa)}\right). \tag{8}$$

Difference and average operators with respect to the other co-ordinates y and t are defined correspondingly. We note that all combinations of these operators are commutative. To abbreviate the expressions further, we also group terms of identical indices inside square brackets, leaving the super- and subscripts outside the bracket. These notations are adopted from Reference 20.

In Reference 11 the set (3) and (4) was discretized exclusively by centred differences and averaging. Hence both the continuity and the Bernoulli equation gave difference equations that were implicit in space. To decouple the implicitness in the two equations, a grid staggered in time was used. This also improves the accuracy significantly for particular combinations of grid increments. The difference equations read

$$[\delta_t \eta = -\delta_x\{(1+\alpha\bar{\eta}^{xt})\delta_x\phi\} - \delta_y\{(1+\alpha\bar{\eta}^{yt})\delta_y\phi\} + \nu C_1]_{i,j}^{(n+1/2)}, \tag{9}$$

$$[\delta_t\phi + T + \eta - \tfrac{1}{3}\varepsilon(\delta_x^2+\delta_y^2)\delta_t\phi + \nu C_2 = 0]_{i,j}^{(n)}, \tag{10}$$

where

$$[T^{(n)} = \tfrac{1}{2}\alpha\{(\delta_x\bar{\phi}^x)^{(n-1/2)}(\delta_x\bar{\phi}^x)^{(n+1/2)} + (\delta_y\bar{\phi}^y)^{(n-1/2)}(\delta_y\bar{\phi}^y)^{(n+1/2)}\}]_{i,j} \tag{11}$$

and νC_1, νC_2 are numerical correction terms that remove second-order errors from the hydrostatic parts of the equations. Thus the overall discretization error is $O(\Delta x^2, \Delta y^2, \Delta t^2)$ for $\nu=0$ and $O(\varepsilon\Delta x^2, \alpha\Delta x^2, \Delta x^4, \varepsilon\Delta y^2, \alpha\Delta y^2, \ldots)$ for $\nu=1$. The correction terms read

$$C_1 = -\tfrac{1}{12}(\Delta x^2+\Delta y^2)\delta_x^2\delta_y^2\phi, \tag{12}$$

$$C_2 = \tfrac{1}{12}(\Delta x^2-\Delta t^2)\delta_x^2\delta_t\phi + \tfrac{1}{12}(\Delta y^2-\Delta t^2)\delta_y^2\delta_t\phi. \tag{13}$$

When ν is set to zero, it is shown in Reference 19 that the difference equations (9) and (10) are equivalent to the following representation of (6) and (5):

$$[\delta_t\eta = -\delta_x\{(1+\alpha\bar{\eta}^{xt})u\} - \delta_y\{(1+\alpha\bar{\eta}^{yt})v\}]_{i,j}^{(n+1/2)}, \tag{14}$$

$$[\delta_t u + \delta_x T = -\delta_x\eta + \tfrac{1}{3}\varepsilon(\delta_x^2+\delta_y^2)\delta_t u = 0]_{i+1/2,j}^{(n)}, \tag{15}$$

$$[\delta_t v + \delta_y T = -\delta_y\eta + \tfrac{1}{3}\varepsilon(\delta_x^2+\delta_y^2)\delta_t v = 0]_{i,j+1/2}^{(n)}, \tag{16}$$

$$[T^{(n)} = \tfrac{1}{2}\alpha\{(\bar{u}^x)^{(n-1/2)}(\bar{u}^x)^{(n+1/2)} + (\bar{v}^y)^{(n-1/2)}(\bar{v}^y)^{(n+1/2)}\}]_{i,j}. \tag{17}$$

These are the constant-depth versions of the difference equations in References 15 and 20.

3. CNOIDAL WAVES

It is well known that the non-linear KdV or Boussinesq equations possess a family of plane and periodic wave solutions of permanent form, generally referred to as cnoidal waves. The solutions are governed by two parameters, the amplitude and wavelength, that determine the shape and frequency. A thorough discussion of cnoidal waves is found in Reference 21. For small ratios α/ε the cnoidal wave solution coincides with the shallow water Stokes wave. The latter solution is found by expanding the field variables and the frequency simultaneously in powers of α. The series for the frequency is achieved by requiring the expansions for the field variables to be consistent and uniformly valid in space and time. Details on the Stokes wave expansion are given in Reference 22.

Assuming no y-dependence and denoting the wave number and frequency by k and ω respectively, we may define the Stokes wave expansion according to

$$\eta = Y_0(\theta) + \alpha Y_1(\theta) + \ldots, \tag{18}$$

$$\phi = Rt + Fx + \Phi_0(\theta) + \alpha\Phi_1(\theta) + \ldots, \tag{19}$$

$$\omega = \omega_0 + \alpha\omega_1 + \alpha^2\omega_2 + \ldots = k(c_0 + \alpha c_1 + \alpha^2 c_2 + \ldots), \tag{20}$$

where $\theta = kx - \omega t$ and the functions Y_j, Φ_j are periodic. We will choose α as the amplitude of the first harmonic of η, which means that $Y_0(\theta) = \cos\theta$. A similar expansion can be applied to the difference equations (9) and (10). We shall not discuss all the details of the tedious and rather straightforward arithmetic, but we note that the calculations are substantially simplified by the following observations and definitions.

(a) The horizontal length scale is chosen according to $l = 1/k^*$, which means that $k = 1$. A new time variable is defined by $\tau = \omega t$. We note that $\delta_t F(\theta) = \omega \delta_\tau F(\theta)$, where $\Delta\tau = \omega\Delta t$.

(b) We define $a_x = (2/\Delta x)\sin(\Delta x/2)$, $m_x = \cos(\Delta x/2)$ and a_τ, m_τ correspondingly to obtain the relations

$$\delta_x \sin\theta = a_x \cos\theta, \qquad \overline{\sin\theta}^x = m_x \sin\theta, \qquad \text{etc.}$$

(c) It is easily shown that

$$\delta_x \sin(2\theta) = 2m_x a_x \cos(2\theta), \qquad \overline{\sin(2\theta)}^x = (2m_x^2 - 1)\sin(2\theta), \qquad \text{etc.}$$

Naturally, in the limit Δx, $\Delta\tau \to 0$ the expansion becomes identical to the analytical one.

3.1. *The linear harmonic solution*

Inserting the series (18)–(20) in (9) and (10), we obtain to leading order

$$Y_0 = \cos\theta, \qquad \Phi_0 = B_0 \sin\theta, \qquad c_0^2 = \frac{a_x^2}{a_\tau^2(1 + \frac{1}{3}\tilde{\varepsilon} a_x^2)}, \tag{21}$$

where $B_0 = c_0 a_\tau / a_x^2$ and $\tilde{\varepsilon} = \varepsilon + \frac{1}{4}\nu(\Delta t^2 - \Delta x^2)$. The expression for c_0 is naturally the discrete linear dispersion relation. By restoring the grid increments into the right-hand side and adopting the scaling according to equation (2), we obtain the stability criterion

$$\Delta\hat{t}^2 \leqslant \Delta\hat{x}^2 + \frac{4}{3 - \nu} \tag{22}$$

and the leading numerical dispersion terms according to

$$\hat{\omega} = \hat{k}\{1 - \tfrac{1}{6}\hat{k}^2 - \tfrac{1}{24}(1 - \nu)(\Delta\hat{x}^2 - \Delta\hat{t}^2)\hat{k}^2 + O(\hat{k}^4)\}. \tag{23}$$

We observe that leading numerical error terms enter the expression to the same order in $\hat{k}$ as the dispersion terms. This is relevant for the choice of scaling indicated by equation (37) in Section 4.

3.2. *The superharmonics*

To the next order we have to apply additional conditions to obtain a unique solution. When the averaged surface elevation and horizontal mass flux are prescribed to be zero, we find

$$c_1 = 0, \qquad Y_1 = A_1 \cos(2\theta), \qquad \Phi_1 = B_1 \sin(2\theta) + R_1 \tau + F_1 x, \tag{24}$$

where

$$A_1 = \frac{1}{4} \frac{m_x^4 + 2m_\tau^2 + \frac{8}{3}\tilde{\varepsilon} m_x^2 m_\tau^2 a_x^2}{m_\tau^2 - m_x^2 + \frac{1}{3}\tilde{\varepsilon}(m_x^2 - 1)a_x^2 m_x^2}, \tag{25}$$

$$B_1 = \frac{c_0 a_\tau m_\tau m_x^2}{4a_x^2} \frac{(\frac{3}{2} + \frac{1}{3}\tilde{\varepsilon} a_x^2)}{m_\tau^2 - m_x^2 + \frac{1}{3}\tilde{\varepsilon}(m_x^2 - 1)a_x^2 m_x^2}, \tag{26}$$

$$R_1 = \tfrac{1}{4} a_x^2 m_x^2 (2m_x^2 - 1), \tag{27}$$

$$F_1 = \tfrac{1}{2} B_0. \tag{28}$$

It is emphasized that the appearance of the coefficient R_1 is related to the choice of the constant in the Bernoulli equation. Letting $\Delta\tau$, $\Delta x \to 0$, we find $\alpha A_1 \to O(\alpha\varepsilon^{-1})$. Hence the expansion is meaningful only if $\varepsilon \gg \alpha \gg \varepsilon^2$, which implies that the Ursell parameter α/ε has to be small. Assuming $O(\Delta x^2 \Delta\tau^2) \leqslant O(\varepsilon)$, the expression for A_1 can be expanded in orders of Δx^2, $\Delta\tau^2$ to give

$$A_1 = \frac{3 + \hat{k}[\frac{8}{3} + \frac{1}{12}\{(8\nu - 6)\Delta\hat{t}^2 - (8\nu + 6)\Delta\hat{x}^2\} + O(\Delta\hat{x}^4, \Delta\hat{t}^4)]}{\hat{k}^2\{\frac{4}{3} + (1 - \frac{1}{3}\nu)(\Delta\hat{x}^2 - \Delta\hat{t}^2) + O(\Delta\hat{x}^4, \Delta\hat{t}^4)\}} \tag{29}$$

Noting that $\Delta\hat{x} = \Delta\hat{t} = 0$ corresponds to the analytical (non-discrete) case, we observe that, regardless of the wavelength, we must require $\Delta\hat{x}$, $\Delta\hat{t} \ll 1$, or $\nu = 1$ and $\Delta\hat{x} = \Delta\hat{t}$, to reproduce A_1 properly. In dimensional co-ordinates the first requirement corresponds to $\Delta x^* \ll h^*$, etc. We note that the correction terms do not improve the value of A_1 markedly.

4. THE SOLITON SOLUTION

The shallow water solitary wave is a single-crested wave of permanent shape with exponentially decaying tails extending to infinity. The propagation speed is slightly larger than that for infinitely long linear waves. Solitary wave solutions are inherent in the weakly dispersive and non-linear theories corresponding to Boussinesq or KdV equations. Strongly non-linear solutions have been obtained by perturbing the full inviscid set as in References 23, 24 and 32. The solitary wave solution has a large amount of interesting features and mathematics attached to it. Most remarkable is maybe the particle-like collision properties which have motivated the soliton name. Within the weakly non-linear and dispersive approximation, solitons regain their original shapes after interaction. A survey on the theory of shallow water solitons can be found in References 21 and 25. In the present paper we will not attempt to discuss the performance of numerical methods in relation to the interaction behaviour, etc. of solitons. Instead we will confine ourselves to the more basic question of the existence of single-crested waves of permanent shape. Still, we will use the term soliton also for the discrete solutions.

As demonstrated in Section 3, the Stokes wave expansion for the difference equations was, at least principally, as simple as for the differential equations. This is due to the existence of Fourier transforms that are essentially identical for the discrete and the non-discrete case. However, the description of a general wave of permanent form moving in a grid is less straightforward, and the existence of such solutions is far from obvious.

We will start with a brief look at a special case for which the concept of a permanent wave-form carries directly over to the discrete description. When the plane permanent wave-forms $\eta = Y(x - ct)$, $\phi = \Phi(x - ct)$ are substituted into the differential equations (3) and (4), we obtain a set of ordinary differential equations in the composite variable $\theta = x - ct$. But, even though we assume no y-dependence and prescribe $\eta_i^{(j)} = Y(i\Delta x - cj\Delta t)$, etc., the partial difference equations will not degenerate to ordinary ones. To achieve an equation that involves single indices only, we must assume $c\Delta t = \Delta x$, which means that the wave profile moves exactly one space increment per time step. This is an awkward requirement, particularly since c generally has to be found as a part of the solution. Anyway, if we assume $c\Delta t = \Delta x$, define $\theta_j = (j - \gamma)\Delta x + c\gamma\Delta t$ and invoke

$$\eta_i^n = Y(\theta_{i+n}), \qquad \phi_i^{(n+1/2)} = \Phi(\theta_{i+n+1/2}) \tag{30}$$

in (3) and (4), we obtain

$$[cY = (1 + \alpha\bar{Y}^{\theta\theta})U]_i, \tag{31}$$

$$[cU - \tfrac{1}{2}\alpha T - Y - \tfrac{1}{3}c\{\alpha + \tfrac{1}{4}\nu\Delta x^2(c^2 - 1)\}\delta_\theta^2 U = 0]_i, \tag{32}$$

where we have exploited the fact that U and Y vanish at infinity and where U and T are defined according to

$$[\delta_\theta \Phi = U]_i, \qquad T_i = \bar{U}^\theta_{i-1/2}\bar{U}^\theta_{i+1/2}. \tag{33}$$

The ordinary difference equations (31) and (32) together with the conditions at infinity define a non-linear eigenvalue problem for c. This problem is probably solvable by a combination of asymptotic approximations at infinity and a shooting technique. Thus a soliton solution is likely to exist. However, the existence of a solution for this particular choice of grid increments is not a reliable indication for the existence of such solutions in general. We will not pursue this case any further but instead turn to another and more general approach.

Provided $c\Delta t/\Delta x$ is a non-rational number, all grid points are associated with different values $\theta_i^{(j)} = i\Delta x - cj\Delta t$ and the definition of a permanent wave-form is not trivial. A simple definition is to link the existence of a solitary wave to the existence of an analytical function $Y(\theta)$ which satisfies the relation $Y(\theta_i^{(j)}) = \eta_i^{(j)}$ for all i and j. If Y exists it is uniquely determined because the set $\{\theta_i^{(j)}\}$ always has accumulation points.* When an analytic function is substituted in (9) and (10) or in (14)–(17), all differences can be replaced by series of derivatives that are found by Taylor series expansions. Retaining only the leading discretization error terms, we will then find approximate solutions to the resulting differential equations. This corresponds to the first few steps of a perturbation procedure which in principle can be carried out to any order, thereby indicating that discrete solitary wave solutions do exist. However, no proof of convergence of the perturbation series is established.

4.1. The perturbation expansion

When the dependent variables in the difference equations are regarded as grid point values of analytical functions, we may apply Taylor series expansion. Expanding the quantities in (9) and (10) about $(i\Delta x, j\Delta y, (n+\frac{1}{2})\Delta t)$ and $(i\Delta x, j\Delta y, n\Delta t)$ respectively, we deduce the differential equations

$$\begin{aligned}\eta_t + \frac{\Delta t^2}{24}\eta_{ttt} + \frac{\Delta t^4}{1920}\eta_{ttttt} = &-\{(1+\alpha\eta)\phi_x\}_x + D_{(x)} - \{(1+\alpha\eta)\phi_y\}_y + D_{(y)} \\ &- \frac{\nu}{12}(\Delta x^2 + \Delta y^2)\left(\phi + \frac{\Delta x^2}{12}\phi_{xx} + \frac{\Delta y^2}{12}\phi_{yy}\right)_{xxyy} \\ &+ O(\alpha\Delta x^{2i}\Delta y^{2j}\Delta t^{2k}, \Delta x^{2I}\Delta y^{2J}\Delta t^{2K}),\end{aligned} \tag{34}$$

$$\begin{aligned}&\phi_t + \frac{\Delta t^2}{24}\phi_{ttt} + \frac{\Delta t^4}{1920}\phi_{ttttt} + \frac{\alpha}{2}(\phi_x)^2 + \frac{\alpha}{2}(\phi_y)^2 + \eta - \left(\frac{\varepsilon}{3} + \frac{\nu}{12}(\Delta t^2 - \Delta x^2)\right)\phi_{xxt} + R_{(x)} \\ &- \left(\frac{\varepsilon}{3} + \frac{\nu}{12}(\Delta t^2 - \Delta y^2)\right)\phi_{yyt} + R_{(y)} + O(\alpha\Delta x^{2i}\Delta y^{2j}\Delta t^{2k}, \varepsilon\Delta x^{2i}\Delta y^{2j}\Delta t^{2k}, \Delta x^{2I}\Delta y^{2J}\Delta t^{2K}) = 0,\end{aligned} \tag{35}$$

where $i+j+k=2$, $I+J+K=3$ and

$$D_{(x)} = -\frac{\Delta x^2}{12}\phi_{xxxx} - \frac{\Delta x^4}{360}\phi_{xxxxxx} - \frac{\Delta x^2}{24}\alpha\{(\eta\phi_x)_{xxx} + (\eta\phi_{xxx})_x + 3(\eta_{xx}\phi_x)_x\} - \frac{\Delta t^2}{8}(\eta_{tt}\phi_x)_x,$$

$$R_{(x)} = +\frac{\Delta x^2}{6}\alpha\phi_{xxx}\phi_x + \frac{\Delta t^2}{4}\alpha\{\phi_x\phi_{xtt} - (\phi_{xt})^2\} - \left(\frac{\varepsilon}{3} + \frac{\nu}{12}(\Delta t^2 - \Delta x^2)\right)\left(\frac{\Delta x^2}{12}\phi_{xxxxt} + \frac{\Delta t^2}{24}\phi_{xxttt}\right).$$

* Accumulation point in the usual mathematical sense: a point for which we may find arbitrarily close $\theta_i^{(j)}$.

Expressions for $D_{(y)}$ and $R_{(y)}$ are obtained simply by replacing x by y in the above definitions. We seek permanent wave solutions as functions of the composite variable

$$\theta = k(x\cos\psi + y\sin\psi - ct) \tag{36}$$

where ψ is the angle between the x-axis and the direction of wave advance. Prescribing

$$\alpha=\varepsilon, \qquad \Delta x^2 = O(\alpha), \qquad \Delta y^2 = O(\alpha), \qquad \Delta t^2 = O(\alpha), \tag{37}$$

we may assume the expansions

$$\eta = Y(\theta) = Y_0 + \alpha Y_1 + \alpha^2 Y_2 + \dots, \tag{38}$$

$$U \equiv \partial\phi/\partial x = U_0 + \alpha U_1 + \alpha^2 U_2 + \dots, \tag{39}$$

$$k = 1 + \alpha k_1 + \alpha^2 k_2 + \dots, \tag{40}$$

$$c = 1 + \alpha c_1 + \alpha^2 c_2 + \dots. \tag{41}$$

Equation (37) corresponds to rather large grid increments, namely $\Delta x^* \sim h^*$, etc. However, the resolution often has to be very coarse in three-dimensional simulations. According to References 11 and 19, sufficient accuracy may still be achieved by the introduction of simple correction terms, or sometimes by choosing an optimal time step. The simpler case of a more refined grid will be discussed later. The expansion of k is necessary because the shape and length of the soliton, like the speed of propagation, depend on the amplitude. The zeroth-order term of k can be chosen arbitrarily without loss of generality. At $\theta = \pm\infty$ we require $Y = Y' = Y'' = \dots = U = U' = U'' = \dots = 0$. A definition of α can be given by $\max Y_0 = 1$. This definition is not precise unless we add the condition that solutions of the same mathematical form as Y_0 must be excluded from higher-order terms. Substitution into (34), (35) and integration of the former give

$$\begin{aligned} cY = {} & (1+\alpha Y)U + \alpha k^2(\gamma_1 U'' - \gamma_2 c^2 Y'') \\ & + \alpha^2\{\kappa_1 U'''' - \kappa_2 Y'''' + \kappa_3 (YU)'' + \kappa_4 Y''U + \kappa_5 YU''\} + O(\alpha^3), \end{aligned} \tag{42}$$

$$cU - \tfrac{1}{2}\alpha U^2 - Y - \alpha(\tfrac{1}{3} + \mu - \gamma_3 c^2)ck^2 U'' - \alpha^2\{\kappa_6 U'''' + \kappa_7 UU'' - \kappa_8 (U')^2\} + O(\alpha^3) = 0. \tag{43}$$

The coefficients are given by

$$\gamma_2 = \gamma_3 = \frac{\Delta t^2}{24\alpha}, \qquad \gamma_1 = \frac{e_2}{12\alpha}, \qquad \mu = \frac{\nu}{12\alpha}(\Delta t^2 - \Delta x^2\cos^2\psi - \Delta y^2 \sin^2\psi),$$

$$\kappa_1 = \frac{e_4}{360\alpha^2} + \frac{\nu}{144}(\Delta x^2 + \Delta y^2)(\Delta x^2\cos^2\psi + \Delta y^2\sin^2\psi)\cos^2\psi\sin^2\psi,$$

$$\kappa_2 = \frac{\Delta t^4}{1920\alpha^2}, \qquad \kappa_3 = \kappa_5 = \frac{e_2}{24\alpha}, \qquad \kappa_4 = \frac{e_2 + \Delta t^2}{8\alpha}, \qquad \kappa_8 = \frac{\Delta t^2}{4\alpha},$$

$$\kappa_6 = \frac{2e_2 + (3\mu+1)\Delta t^2}{72\alpha} - \kappa_2 + \frac{\nu}{144}\{\Delta x^2(\Delta t^2 - \Delta x^2)\cos^4\psi + \Delta y^2(\Delta t^2 - \Delta y^2)\sin^4\psi\},$$

$$\kappa_7 = \frac{2e_2 + 3\Delta t^2}{12\alpha}, \tag{44}$$

where $e_2 = \Delta x^2\cos^4\psi + \Delta y^2\sin^4\psi$ and $e_4 = \Delta x^4\cos^6\psi + \Delta y^4\sin^6\psi$. The distinctions between coefficients with equal values are kept for generality. Invoking the series expansion and requiring that every order of α shall vanish, we obtain a hierarchy of equations of the form

$$Y_i - U_i = R_i(Y_0 \cdots Y_{i-1}, U_0 \cdots U_{i-1}; \cdots c_i, \cdots k_{i-1}), \tag{45}$$

$$U_i - Y_i = H_i(Y_0 \cdots Y_{i-1}, U_0 \cdots U_{i-1}; \cdots c_i, \cdots k_{i-1}), \tag{46}$$

where $R_0 = H_0 = 0$. This means that, after having computed Y_{j-1}, U_{j-1}, we find Y_j, U_j by solving the set

$$Y_j - U_j = R_j, \qquad R_{j+1} + H_{j+1} = 0. \tag{47}$$

The latter equation is a solubility condition for the next order.

4.2. The zeroth-order solution

For the leading terms of the expansion we obtain $U_0 = Y_0$ and

$$2\sigma Y_0'' + (\tfrac{3}{2} Y_0 - 2c_1) Y_0 = 0, \tag{48}$$

where $\sigma = \frac{1}{2}(\frac{1}{3} + \mu + \gamma_1 - \gamma_2 - \gamma_3)$. Integration of Y_0 times (48) immediately gives

$$\sigma(Y_0')^2 + (\tfrac{1}{2} Y_0 - c_1) Y_0^2 = 0. \tag{49}$$

The above equation together with (48) will be used to remove derivatives of Y_0 from the right-hand side of the higher-order equations. This will work as long as the sum of the number of derivations applied to all factors of each term is even. To avoid negative solitons with negative c_1, we have to require $\sigma > 0$. Anyway, this turns out to be a much weaker condition than the linear stability criterion (22). From the above equation and the constraint max $Y_0 = 1$ we find

$$c_1 = \tfrac{1}{2}, \tag{50}$$

$$Y_0 = \cosh^{-2}\left(\frac{\theta}{2\sqrt{(2\sigma)}}\right). \tag{51}$$

A few important observations should be made at this stage. We note that to order α the propagation speed c is independent of the discretization whereas the shape of the soliton is not. In fact, even an erroneous factor before the dispersion term will not alter c to this order. Therefore considerations on propagation speeds of solitons alone should never be used to validate numerical methods.

The quantity σ has a simple interpretation. If the non-linear term of (48) is omitted, the equation must describe linear solutions of permanent form, which means sinusoidal waves. In this case the perturbation parameter α has to be regarded as a measure of wavelength instead of amplitude. To get a unique definition of the parameter, we demand that the dimensionless wave number equals unity and find $c_1 = -\sigma$, which means

$$c = 1 - \sigma(k^* h_0)^2 + O((k^* h_0)^4). \tag{52}$$

The analysis in the present section has so far been concerned only with the difference formulation (9) and (10), alternatively (14) and (15). However, any consistent and regular discretization of the Boussinesq equations will lead to a zeroth-order solution of the form (51) with σ having the above interpretation. A consequence is that the zeroth-order solution for the discrete solitary wave can be deduced from the linear hydrostatic dispersion relation. (The 'analytical part' of σ is always $\frac{1}{6}$.) This is different for KdV or KP equations which are expressed in terms of a composite variable $x - t$ in addition to a slow time variation.

We note that to the present order all numerical errors disappear when the correction terms are retained ($\nu=1$) or if $\Delta t^2=\Delta x^2\cos^4\psi+\Delta y^2\sin^4\psi$. In these cases the difference equations are accurate to the same order as the Boussinesq equations provided that (37) holds.

4.3. *The first-order solution*

Most of the important features of discrete solitons are revealed by the leading terms alone. In fact, the $O(\alpha\varepsilon, \varepsilon^2)$ error terms of the Boussinesq equations themselves would enter the perturbation scheme at the next stage. Still, we will advance the perturbation expansion one step further to indicate the *existence* of solitary wave solutions of the set (9) and (10). Besides, it is essential for the verification of numerical methods and programmes to have as precise descriptions as possible of both analytical and numerical solutions, even though the accuracy of the basic theory is limited. Rewriting R_1, R_2 and H_2 from equations (45) and (46), repeatedly using (48) and (49) to remove derivatives of Y_0 and finally eliminating U_1, we obtain an equation of the form

$$L(Y_1)\equiv 2\sigma Y_1''+(3Y_0-1)Y_1=aY_0+bY_0^2+fY_0^3, \tag{53}$$

where

$$a=2c_2-2k_1-\tfrac{3}{4}+\tfrac{1}{2}\sigma^{-1}(\gamma_1-\tfrac{1}{2}\gamma_2+\gamma_3)+\tfrac{1}{4}\sigma^{-2}\gamma_2(\gamma_1-\gamma_2)-\tfrac{1}{4}\sigma^{-2}(\kappa_1-\kappa_2+\kappa_6), \tag{54}$$

$$\begin{aligned}b=3k_1+4+\sigma^{-1}(-\tfrac{11}{4}\gamma_1+\tfrac{35}{8}\gamma_2-\tfrac{3}{4}\gamma_3)-\tfrac{1}{2}\sigma^{-1}(4\kappa_3+\kappa_4+\kappa_5+\kappa_7-\kappa_8)\\ -\tfrac{15}{8}\sigma^{-2}\gamma_2(\gamma_1-\gamma_2)+\tfrac{15}{8}\sigma^{-2}(\kappa_1-\kappa_2+\kappa_6),\end{aligned} \tag{55}$$

$$\begin{aligned}f=-3+\sigma^{-1}(\tfrac{9}{4}\gamma_1-\tfrac{19}{4}\gamma_2)+\tfrac{3}{4}\sigma^{-1}(\tfrac{10}{3}\kappa_3+\kappa_4+\kappa_5+\kappa_7-\kappa_8)\\ +\tfrac{15}{8}\sigma^{-2}\gamma_2(\gamma_1-\gamma_2)-\tfrac{15}{8}\sigma^{-2}(\kappa_1-\kappa_2+\kappa_6).\end{aligned} \tag{56}$$

In contrast to (48), equation (53) is linear, but inhomogeneous, and has variable coefficients. However, by differentiating (48), it is immediately realized that $V=Y_0'$ is a solution of the homogeneous equation $L(V)=0$. The other homogeneous solution grows exponentially as $\theta\rightarrow\pm\infty$. If $H^{(j)}$ is defined as the symmetric and finite solution of $L(V)=Y_0^j$, it is easily shown that

$$H^{(1)}=\tfrac{1}{2}\theta Y_0'+Y_0, \qquad H^{(2)}=\tfrac{2}{3}Y_0,$$

$$H^{(j+1)}=\frac{1}{3-\tfrac{1}{2}j-j^2}\{Y_0^j-(j^2-1)H^{(j)}\}, \quad j\geqslant 2. \tag{57}$$

For Y_1 we thus find

$$Y_1=\beta Y_0'+a(\tfrac{1}{2}\theta Y_0'+Y_0)+(\tfrac{2}{3}b+f)Y_0-\tfrac{1}{2}fY_0^2. \tag{58}$$

The first term on the right-hand side corresponds to a constant phase shift of order α in Y_0. Thus requiring that the maximum shall be located at $\theta=0$ to all orders yields $\beta=0$. The second term violates the uniformity of the expansion (secular term) and we must have $a=0$. Finally, the third term only modifies the definition of α and must be prescribed to vanish to give unique values for c_2 and k_1. This gives

$$Y_1=-\tfrac{1}{2}fY_0^2. \tag{59}$$

For a more refined grid we may assume that the increments are of order α instead of $\alpha^{1/2}$. In this case the discretization errors will first appear in the equations for Y_1 and U_1 and only cause a modification of k_1. We shall not go into details but merely state that when the grid increments are restored into (51), the resulting expression is valid also in this case.

4.4. Higher-order terms

Provided sufficient terms from the Taylor series expansion are retained in (34) and (35), the expansion can be carried out to any order, although the arithmetic becomes unbearable. It is easily realized that only terms of even derivatives will enter the counterparts of (42) and (43). For product terms the sum of the derivatives of each factor has to be even. We may then recursively obtain equations of the form

$$L(Y_n)=\sum_{i=1}^{n+2} a_i^{(n)} Y_0^i, \tag{60}$$

where $a_1^{(n)}$ and $a_2^{(n)}$ are functions of $c_{(n+1)}$ and k_n. This equation can be handled in the same manner as (53). Solutions Y_n that vanish at infinity can thus be found for all n. Formally, the total solution for Y will become a power series in Y_0. We note that the a_1-coefficients stem exclusively from the linear parts of the equations. Thus requiring these coefficients to be zero must correspond to some dominant balance between linear terms. Since the solutions have the form of power series in Y_0, the behaviour at the outskirts of the soliton will be

$$\eta\sim 4\exp\left(-\frac{|\theta|}{\sqrt{(2\sigma)}}\right), \qquad \phi\sim 4B\exp\left(-\frac{|\theta|}{\sqrt{(2\sigma)}}\right), \tag{61}$$

which means that the linear terms have to dominate at infinity. Substituting the above expressions into the linearized versions of (9) and (10), we find

$$\Omega^2(1-\tfrac{1}{3}\alpha K^2)=K^2, \qquad B=-\Omega K^{-2}, \tag{62}$$

where

$$K=\frac{2}{\Delta x}\sinh\left(\frac{k\Delta x}{2}\right), \qquad \Omega=\frac{2}{\Delta t}\sinh\left(\frac{kc\Delta t}{2}\right). \tag{63}$$

Exploiting this relation and invoking the power series directly in the equations corresponding to (34) and (35) will simplify the arithmetic to some extent. Still, we have no intention of calculating the higher Y_n. Neither will we attempt to derive bounds on the higher-order coefficients, thereby leaving the question of convergence open. Anyway, one limitation of the present theory has now become apparent. The whole approach depends on the convergence of the Taylor series expansion in (34) and (35). Hence we must require that $k\Delta x\cos\psi$, $k\Delta y\sin\psi$ and $kc\Delta t$ be less than the radius of convergence of the Taylor series belonging to Y_0. This radius equals $\pi\sqrt{(2\sigma)}$. For larger grid increments a discrete soliton, defined through an analytical interpolant, may still exist, but it cannot be found by the present procedure.

4.5. Verification and comparison with simulation

In the present subsection it is more convenient to describe the solitary waves in terms of the total wave height A instead of the perturbation parameter α. We will also introduce the renormalized quantities $\hat{x}$, $\hat{t}$ and $\hat{\eta}$, which are defined at the beginning of Section 2, and confine the discussion to two-dimensional cases. The exact solution will be denoted by $\hat{\eta}_{(e)}$ for the analytical (non-discrete) as well as the discrete case. Correspondingly, $\hat{\eta}_{(0)}$ and $\hat{\eta}_{(1)}$ denote the two lowest levels of approximation. Naturally, the perturbation expansion described in Sections 4.1–4.3 is applicable also to the analytical case, just by putting $\Delta x=\Delta t=0$.

The zeroth-order approximation to a soliton of height A is defined as

$$\hat{\eta}_{(0)}=AY_0(\theta), \qquad \theta=\sqrt{(A)}(\hat{x}-c\hat{t}), \qquad c=1+\tfrac{1}{2}A. \tag{64}$$

Correspondingly, the first-order approximation is given by

$$\hat{\eta}_{(1)} = \alpha Y_0(\theta) - \tfrac{1}{2}\alpha^2 f Y_0(\theta)^2, \qquad \theta = (1+\alpha k_1)\sqrt{(\alpha)}(\hat{x} - c\hat{t}), \qquad c = 1 + \tfrac{1}{2}\alpha + c_2\alpha^2, \tag{65}$$

where $\alpha(A)$ is a solution of

$$A = \alpha - \tfrac{1}{2} f\alpha^2. \tag{66}$$

The above definitions imply that the height of the soliton becomes correct whereas the length, shape and speed will display deviations.

Letting Δx, $\Delta t \to 0$, we find by some simple manipulations that

$$c = 1 + \tfrac{1}{2}A - \tfrac{5}{24}A^2 + O(A^3), \tag{67}$$

which is consistent with the result of Reference 19. In Figure 1 we have compared the analytical $\hat{\eta}_{(0)}$ and $\hat{\eta}_{(1)}$ with the 'exact' soliton solution $\hat{\eta}_{(e)}$ of the set (3) and (4). This solution is obtained by accurate numerical integration as described in Reference 11. Naturally, a similar procedure of solution is not available for the discrete case. Even though $A = 0{\cdot}5$ is a large amplitude and clearly outside the validity range of the Boussinesq equations, both approximations agree well with $\hat{\eta}_{(e)}$.

To confirm the validity of the perturbation expansion in the discrete case, we have compared $\hat{\eta}_{(0)}$ and $\hat{\eta}_{(1)}$ with solutions of the difference equations (9) and (10) that are assumed to be solitons. These solutions are generated by evolution from initial conditions. The corresponding analytical case is thoroughly analysed by the inverse scattering technique.[21] If the leading pulse that evolves reaches a permanent state, we accept this as a soliton solution. In the computer calculations the exponentially decaying head and tail of the soliton have to be truncated, and care must be taken to avoid this influencing the solution. When a soliton solution of (3) and (4) is used as initial conditions, we find that the amplitude A changes slowly in time. Meanwhile a trough and a dispersive tail evolve. In Figure 2 we have displayed $A(\hat{t})$ for $A_0 \equiv A(0) = 0{\cdot}1$ and $A_0 \equiv A(0) = 0{\cdot}3$. Both functions clearly seem to approach a finite limit as $\hat{t} \to \infty$. The fluctuations, which are particularly noticeable for $A_0 = 0{\cdot}3$, are due to the spline interpolation used to find $A(\hat{t})$. Such an interpolation is sensitive to the location of the maximum relative to the nearest grid point. In Figure 3 we have compared the calculated wave profiles with the various soliton solutions. The agreement between the discrete solution and $\hat{\eta}_{(1)}$ is nearly perfect. These results strongly support the relevance of the perturbation solution.

When the correction terms are retained ($v = 1$), we still get a noticeable decrease in amplitude relative to A_0. This is partly due to the initial conditions, which are not corrected. Anyway, the

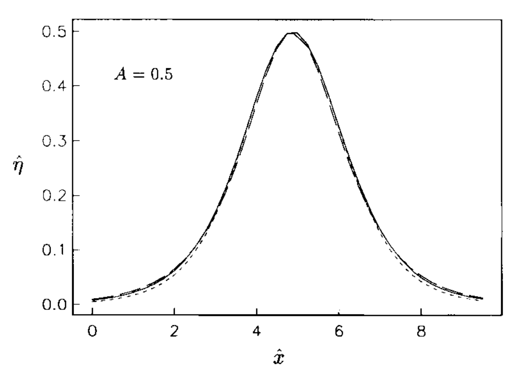

Figure 1. Wave profiles for $\Delta\hat{x} = \Delta\hat{t} = 0$ and $A = 0{\cdot}5$: long dashes, exact solution ($\hat{\eta}_{(e)}$) of the differential equations; full line, first-order solution ($\hat{\eta}_{(1)}$); short dashes, zeroth-order solution ($\hat{\eta}_{(0)}$)

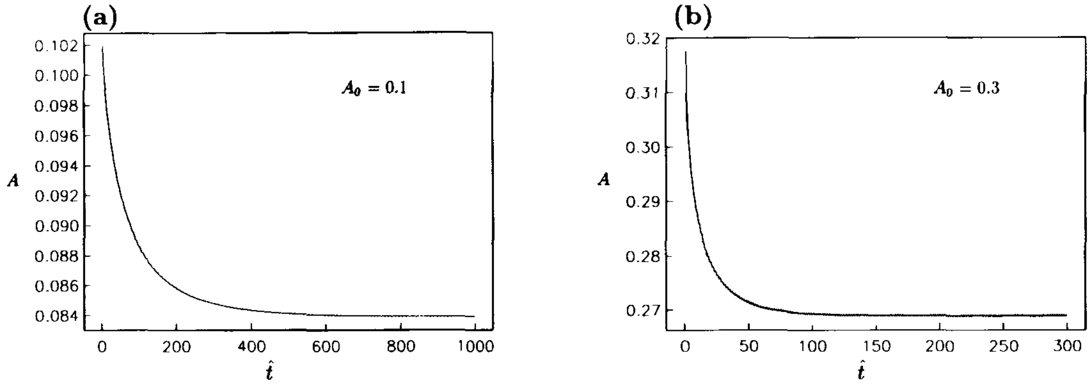

Figure 2. Wave height, A as function of time when (9) and (10) are solved with an 'exact' solitary wave solution as initial state: (a) $A_0=0{\cdot}1$, $\Delta\hat{x}=1{\cdot}5$, $\Delta\hat{t}=0{\cdot}5$; (b) $A_0=0{\cdot}3$, $\Delta\hat{x}=1{\cdot}0$, $\Delta\hat{t}=0{\cdot}3$

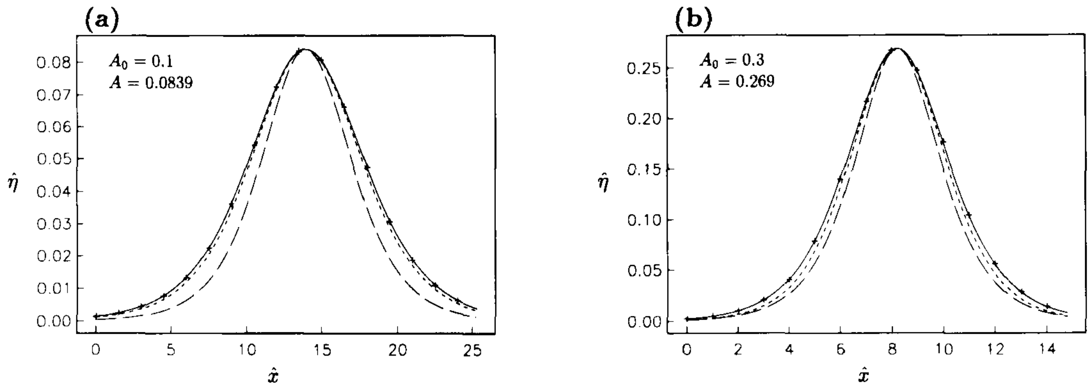

Figure 3. Wave profiles. The crosses correspond to values of the surface elevation at the grid points, the full line and the short dashes to the discrete $\hat{\eta}_{(0)}$ and $\hat{\eta}_{(1)}$ respectively and the long dashes to the exact soliton solution of the differential equations. The location of the origin has no relevance. (a) $A_0=0{\cdot}1$, $\Delta\hat{x}=1{\cdot}5$, $\Delta\hat{t}=0{\cdot}5$, $\hat{t}=1000$; (b) $A_0=0{\cdot}3$, $\Delta\hat{x}=1{\cdot}0$, $\Delta\hat{t}=0{\cdot}3$, $\hat{t}=300$

crucial point is that the wave profile which eventually evolves is much closer to the exact one than for $\nu=0$. This is illustrated in Figure 4 which displays profiles for the same set of parameters as Figure 3(a). The improvement of the numerical solution (crosses) is substantial. The deviation between the discrete solution and $\hat{\eta}_{(1)}$ is still small, but noticeably larger than in the previous cases. Other comparisons have revealed that the accuracy of the perturbation solution becomes poorer when the correction terms are nearly equal to the dispersion terms. A moderate reduction of the grid increments causes $\hat{\eta}_{(1)}$ and the discrete solution to once again coincide almost exactly, as shown in Figure 5.

4.6. *Three-dimensional solutions*

In computer calculations, solitons of oblique orientation relative to the grid axes generally must be treated as fully three-dimensional waves. It is possible to simulate only a finite length of the crest and some non-trivial conditions have to be applied at the lateral boundaries. The

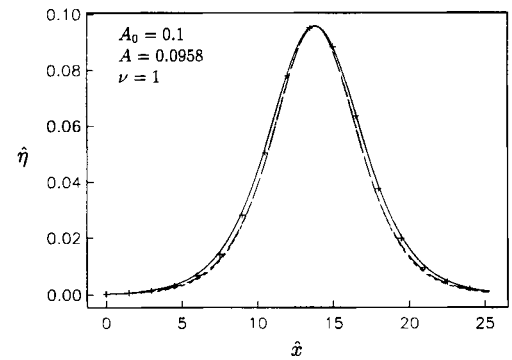

Figure 4. Wave profile for $\nu = 1$ and the same grid increments as in Figure 3(a)

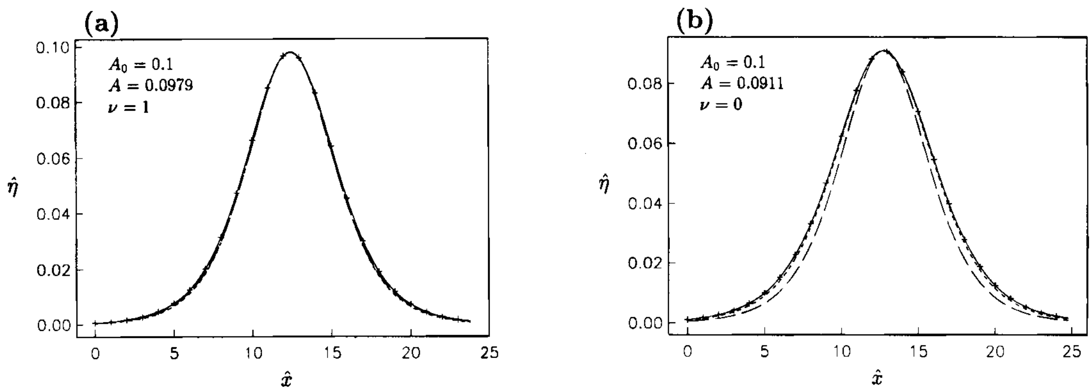

Figure 5. Wave profiles at $\hat{t} = 1000$ for $A_0 = 0{\cdot}1$, $\Delta\hat{x} = 1{\cdot}0$ and $\Delta\hat{t} = 0{\cdot}2$: (a) $\nu = 1$; (b) $\nu = 0$. The interpretation of the lines and crosses is as in Figure 3

outcome of such calculations may be influenced at least as much by these conditions as by the difference discretization itself. Thus the question of the existence of oblique solitons cannot easily be answered through studies of the evolution from initial conditions alone. We may state that whereas the discrete perturbation solution made conclusions concerning the 2D case firmer, more general and easier to reach, a proper discussion of the 3D solitons might rely mainly on the closed-form solution. A special case is given by $\tan\psi = \Delta x/\Delta y$, for which the discrete equations (3) and (4) reduce to their two-dimensional form with $\Delta x \cos\psi$ as the new space increment.

There are no noticeable differences between the cases $\psi = 0$ and $\psi \neq 0$ as far as the perturbation expansion is concerned. Therefore it is likely that oblique soliton solutions also exist and are closely approximated by $\hat{\eta}_{(1)}$. Still, we will report on a single oblique soliton solution of (9) and (10). Even though we have chosen one of the simplest cases possible, a proper description will be rather long and rich in details concerning the physics. Therefore we leave the discussion of the simulation for the Appendix. The final result of the calculation corresponds to a soliton defined by $A = 0{\cdot}0865$ and $\psi = 30{\cdot}6°$, discretized on a grid with increments $\Delta x = 1{\cdot}5$, $\Delta y = 2{\cdot}5$ and $\Delta t = 0{\cdot}5$ without correction terms. As shown in Figure 6, the agreement between the perturbative representation and the 'exact discrete' solution is again excellent. In Figure 7 we have compared

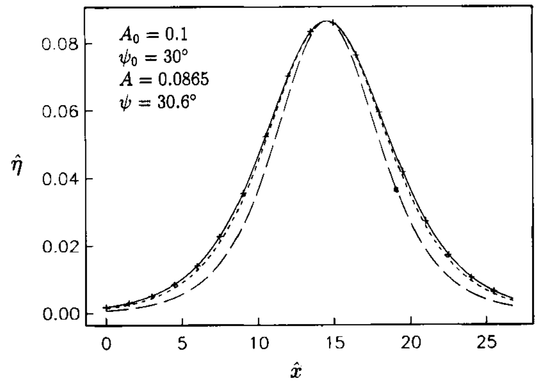

Figure 6. Cross-sections parallel to the x-axis of an oblique solitary wave for $\psi = 30{\cdot}6°$. The notation is as in Figure 3

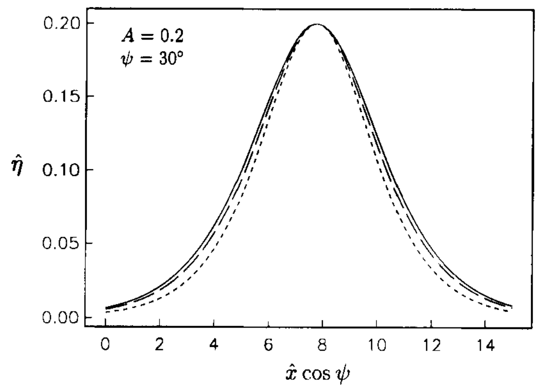

Figure 7. Soliton profiles for $\psi = 30°$. **The units on the co-ordinate axis correspond to dimensionless length along the direction of wave advance. Full line, $\hat{\eta}_{(1)}$ for $\nu = 1$; short dashes, $\hat{\eta}_{(1)}$ for $\nu = 0$, $\Delta\hat{x} = \Delta\hat{t} = 1{\cdot}5$, $\Delta\hat{y} = 1{\cdot}0$; long dashes, exact solution of the differential equations**

the approximate discrete solutions $\hat{\eta}_{(1)}$, with and without correction terms, with the full analytical solution $\hat{\eta}_{(e)}$ for a slightly larger amplitude and a different discretization. The improvement due to the correction term ($\nu = 1$) is apparent but will be more pronounced for smaller amplitudes and less coarse grids.

4.7. Asymmetric difference representations

The use of upwind differences for convective terms or any sort of explicitness in the time stepping will violate the symmetry of the difference equations. Generally, implicit equations such as (9) and (10) must be solved by some iterative technique. This may, at least in principle, introduce asymmetry. The effect of upwinding or iteration will often be numerical dissipation, which makes the existence of permanent wave-forms unlikely. However, neither the Boussinesq equations (3) and (4) nor their numerical counterparts are exactly energy-conserving and solitary waves do still exist. In view of this the question of the existence of solitons for weakly asymmetric cases calls for a more careful discussion. Besides, it would be instructive to see how the perturbation scheme from the previous sections eventually fails.

In Reference 11 the continuity equation (9) is solved by pointwise iteration. If only one iteration is used, this method corresponds to an explicit representation of the non-linear term yielding an error of order $\alpha\Delta t$. Even though this error is comparatively small, it causes a noticeable growth in amplitude which rapidly makes the results worthless. Even the application of two iterations yield a very small, but observable, amplification which indicates that no permanent wave-form evolves. This is demonstrated in Figure 8 which also shows that the use of four iterations gives no apparent growth for the displayed time interval ($\hat{t}<3000$). The use of n iterations will give second-order accuracy provided $n>1$, but will also introduce an error of order Δt^{2n+1} in (34) which corresponds to a term of order $\alpha^{n+1/2}$ in (42). One implication is that we have to expand in half-powers of α, even though the half-powers less than n will vanish. Another is that at stage $n+\frac{1}{2}$ we obtain an equation

$$L(Y_{n+1/2})=q(Y_0, c_{n+1/2}, k_{n-1/2})+F, \tag{68}$$

where q is a quadratic function of Y_0 and F is an odd function in the sense that $F(\theta)=-F(-\theta)$. The odd term stems from the $O(\alpha^{n+1/2})$ term in the counterpart of (42) which involves an odd

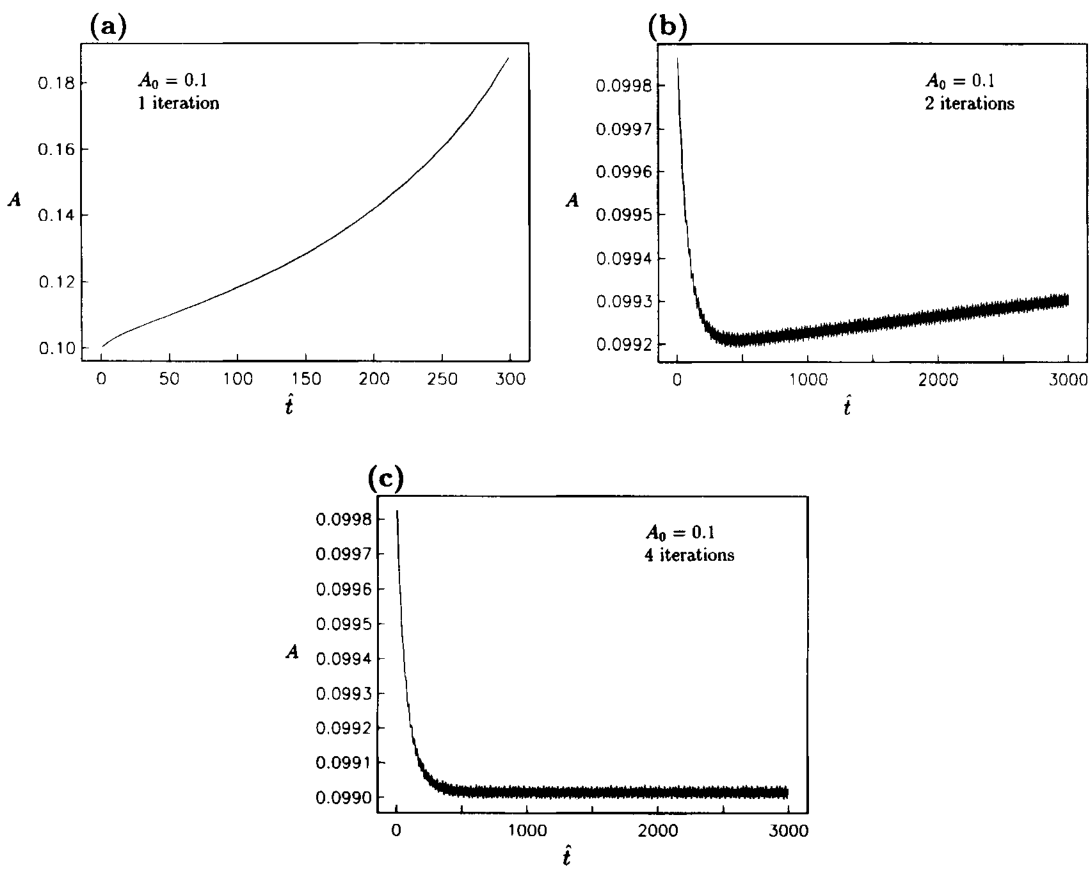

Figure 8. Time histories for the maximum wave height when pointwise iteration is used. The grid increments are $\Delta\hat{x}=\Delta\hat{t}=1{\cdot}0$ for all cases

number of derivations. However, no solution of (68) can vanish at both $\theta=+\infty$ and $\theta=-\infty$ unless the right-hand side is even in θ. As a consequence the perturbation expansion breaks down. To prove the statement concerning (68), we multiply both sides by Y_0', integrate from $\theta=-\infty$ to $\theta=+\infty$, apply integration by parts to the left-hand side and finally invoke equation (48) to obtain

$$\{2\sigma Y_0' Y_{n+1/2}' + (\tfrac{3}{2}Y_0 - 1)Y_0 Y_{n+1/2}\}\big|_{-\infty}^{+\infty} = \int_{-\infty}^{+\infty} F Y_0' \,\mathrm{d}\theta \geqslant 0. \tag{69}$$

For non-zero F this equation can be satisfied only if

$$Y_{n+1/2} \sim \exp\left(\frac{|\theta|}{\sqrt{(2\sigma)}}\right) \tag{70}$$

at $\theta=\infty$ or $\theta=-\infty$. We may conclude that the soliton solution is violated for any finite number of iterations. Still, if n is large, the higher-order imperfection in the expansion will be noticeable only for extremely large times. For the present pointwise iteration scheme the growth in amplitude is so weak that even $n=2$ will suffice in most cases. However, for the calculations on steady ship wave patterns in Reference 11 the effect of using only two iterations was noticeable and n was increased to $n=5$. The actual calculations involved slow energy exchange between (near-) solitons and were carried out for large time intervals.

From the above discussion it also follows that upwind differences will ruin the solitary wave solution. This is not the case for line-by-line iterations as described in References 11, 19 and 20, which do not introduce odd error terms. The use of any kind of smoothing will, on the other hand, introduce damping, which again may distort the soliton solution.

5. CONCLUSIONS

By applying perturbation expansions to the difference equations (9) and (10), we have established formal power series solutions corresponding to the cnoidal and the solitary wave. For the solitary wave the validity of the approach has been demonstrated by comparison between a two-term approximation and the full (or presumably exact) solution, although no rigorous proof of convergence is given. The full solution is obtained by accurate numerical integration for the differential equations and by time evolution of a steady permanent wave-form in the discrete case. We conclude that discrete solitary waves do exist.

Quantitatively, the perturbation solution shows that the phase speed becomes accurate regardless of the discretization and sometimes even of the consistency of the numerical method. As a consequence the propagation speed of solitary waves cannot be used for the validation of numerical methods. The discrete closed-form solution also reveals that the inclusion of simple correction terms improves the accuracy substantially for coarse grids. This is confirmed by computer calculations. Particularly useful is the information the series solution gives on the accuracy of representations of solitons that are oblique in the sense that the direction of wave advance does not coincide with any of the grid axes. A proper investigation of the existence and accuracy of such discrete waves would be extremely difficult without access to 'handmade' solutions of the difference equations.

The accurate representation of the second harmonic of a cnoidal wave requires a refined grid mesh. This result is confined to small Ursell numbers; for moderate and high Ursell numbers the behaviour will probably be as for solitary waves.

The methods used are immediately applicable to any symmetric and homogeneous difference or element discretization. By symmetric we mean that *all* error terms are of even order in the grid increments. On the other hand, if the symmetry is violated by iterative equation solvers, upwinding, predictor–corrector representations, etc., the perturbation expansion collapses. This is demonstrated for a case involving pointwise iteration. It is also shown that the absence of a perfect solitary wave solution is of no consequence unless the number of iterations is very small. Generally, the acceptable level for damping of the 'imperfect solitons' depends on the other time scales of the actual problem. Anyway, the question of the existence or damping rates of near-solitons should always be considered when studying the development of steady state solutions or related problems.

APPENDIX: A SIMULATION WITH AN OBLIQUE WAVE

Owing to increased CPU time and storage demands, it is always a heavier task to perform good test simulations in two than in one space dimension. In the present work this aspect is accentuated through the need for long evolution scales and restrictions concerning the truncation of the exponentially decaying tails of the soliton. Even more important, maybe, is the increased complexity of the dynamics of a crest in three dimensions. As will be discussed below, non-linear refraction effects may confuse the results as well as make the boundary value problems ill-posed.

A computational domain is defined by $\hat{x}_0(t)<\hat{x}<\hat{x}_0(t)+L$ and $0<\hat{y}<B$. At $\hat{y}=0$ we specify $\hat{\phi}$ and the normal derivative of $\hat{\eta}$ according to the analytical soliton solution of amplitude A_0 and incidence ψ_0. For small $\hat{t}$ we also specify the wave at $\hat{x}=\hat{x}_0$. To keep the crest within the calculation window, we have introduced the position $\hat{x}_0$ as a time-dependent function that increases with a multiple of $\Delta\hat{x}$ whenever needed. At $\hat{y}=B$ we apply the radiation condition that has been previously used in Reference 11.

We must expect that both A and ψ will be slowly varying functions of $\hat{y}$ and $\hat{t}$. Our hope is that the solution will reach a permanent state for $\hat{t}\to\infty$ and that this steady solution will display a domain close to $\hat{y}=B$ where the wave characteristics do not vary noticeably with $\hat{y}$. The amplitude A is found for each grid row by spline interpolation as in the two-dimensional case. Applying a polynomial least-squares fit to the locations of the maxima in each row, we then extract values for the orientation ψ. As will be apparent, the calculated ψ will be much more sensitive to interpolation errors than A. This is mainly due to the lesser accuracy for the location of the maximum points. Since the accuracy will depend on the crest location relative to the nearest grid lines, the values for A and ψ will display nearly periodic fluctuations in $\hat{y}$ and $\hat{t}$.

The appropriate choices for B, L and the time of integration call for a careful discussion. If we invoke the concept of rays, we may define a total time of propagation according to the length of the ray sections confined within $0<\hat{y}<B$. If we assume that the variations of ψ and A are small, this time, i.e. the time available for evolution towards a steady state, becomes $t_r=B\cot(\psi_0)/c$. For similar amplitudes and grid increments, t_r should be as large as the integration times used in Section 4.5. The value of t_r gives an indication as to the size of B and, consequently, of L, but it will not determine the time of integration. It is shown in the literature[1,26–29] that a soliton-like crest is subjected to non-linear refraction effects in the form of perturbations on A and ψ. These perturbations propagate laterally along characteristics, C^+ and C^- with approximate speeds $U^+=c\tan\psi+\sqrt{(A/3)}$ and $U^-=c\tan\psi-\sqrt{(A/3)}$ respectively. Thus, as long as $c\tan\psi>\sqrt{(A/3)}$, all perturbations are swept in the positive y-direction and leave the computational domain at $\hat{y}=B$. The time of integration then has to be larger than $t_c=B/U^->t_r$. If, on the other hand, $U^-<0$, disturbances from the interior and the radiation condition may propagate in the negative y-direction along C^- and violate the input condition at $\hat{y}=0$. A stationary pattern may of course still evolve, but the opposite is also conceivable. Anyway, much effort and care have to be devoted

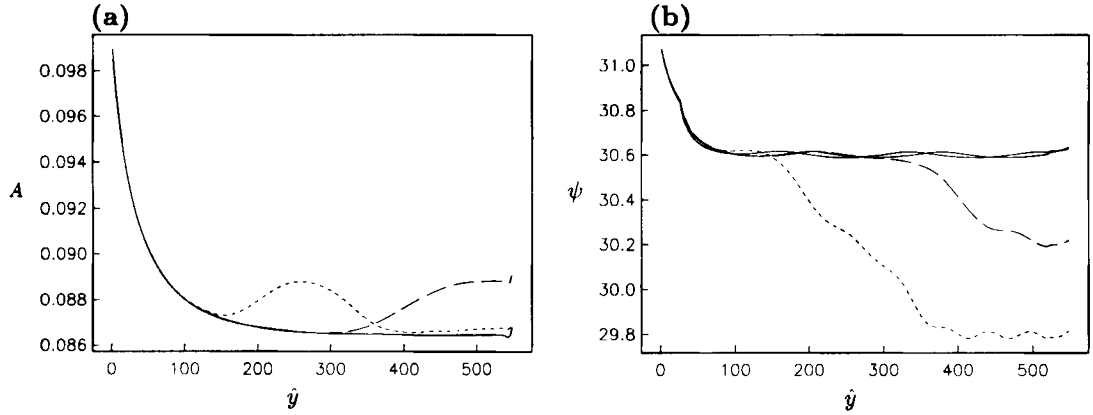

Figure 9. (a) Amplitude and (b) inclination as functions of $\hat{y}$ at different instants: short dashes, $\hat{t}=540$; long dashes, $\hat{t}=1080$; full line, $\hat{t}=1820$, 2080

to the construction of boundary conditions as well as interpretations of the results. Also, the integration times have to be very large.

We will avoid the confusing case $U^- < 0$ by choosing $\psi_0 = 30°$ and $A_0 = 0{\cdot}1$. The grid increments are $\Delta\hat{x} = 1{\cdot}5$, $\Delta\hat{y} = 2{\cdot}5$, $\Delta\hat{t} = 0{\cdot}5$ and the size of the domain is given by $B = 550$, $L = 375$. Wave heights A and inclinations ψ are shown as functions of $\hat{y}$ for selected times $\hat{t} = 540$, 1080, 1820, 2080 in Figure 9. For the first two instants we notice a refraction pattern moving towards $\hat{y} = B$. In spite of the persistent oscillations for ψ, it seems clear that a stationary crest evolves and that we have negligible spatial variations for $400 < \hat{y} < 500$, say. The cross-section at $\hat{y} = 500$ and $\hat{t} = 2080$ is displayed in Figure 6.

REFERENCES

1. R. Grimshaw, 'The solitary wave in water of variable depth. Part 2', *J. Fluid. Mech.*, **46**, 611–622 (1971).
2. R. S. Johnson, 'On the development of a solitary wave moving over an uneven bottom', *Proc. Camb. Phil. Soc.*, **73**, 183–203 (1973).
3. C. J. Knickerbocker and A. C. Newell, 'Shelves and the Korteweg–de Vries equation', *J. Fluid Mech.*, **98**, 803–818 (1980).
4. C. J. Knickerbocker and A. C. Newell, 'Reflections from solitary waves in channels of decreasing depth', *J. Fluid Mech.*, **153**, 1–16 (1985).
5. G. Pedersen and B. Gjevik, 'Run-up of solitary waves', *J. Fluid Mech.*, **135**, 283–299 (1983).
6. D. H. Peregrine, 'Long waves on a beach', *J. Fluid Mech.*, **27**, 815–817 (1967).
7. R. C. Ertekin, W. C. Webster and J. V. Wehausen, 'Ship-generated solitons', *Proc. 15th Symp. on Naval Hydrodynamics*, Hamburg, 1984, pp. 347–364.
8. R. C. Ertekin, W. C. Webster and J. V. Wehausen, 'Waves caused by a moving disturbance in a shallow channel of finite width', *J. Fluid Mech.*, **169**, 275–292 (1986).
9. C. Katsis and T. R. Akylas, 'On the excitation of long nonlinear water waves by a moving pressure distribution. Part 2. Three-dimensional effects', *J. Fluid Mech.*, **177**, 49–65 (1987).
10. C. C. Mei, 'Radiation of solitons by slender bodies in a shallow channel', *J. Fluid Mech.*, **162**, 53–67 (1986).
11. G. Pedersen, 'Three-dimensional wave patterns generated by moving disturbances at transcritical speeds', *J. Fluid. Mech.*, **196**, 39–63 (1988).
12. D. M. Wu and T. Y. Wu, 'Three-dimensional nonlinear long waves due to moving surface pressure', *Proc. 14th Symp. on Naval Hydrodynamics*, 1982, pp. 103–129, National Academy Press, Washington, D.C., 1983.
13. M. B. Abott, H. M. Petersen and O. Skovgaard, 'On the numerical modelling of short waves in shallow water', *J. Hydrol. Res.*, **16**, 173–203 (1978).
14. M. B. Abott, A. D. McCowan and I. R. Warren, 'Accuracy of short-wave numerical models', *J. Hydraul. Eng.*, **110**, 1287–1301 (1985).

15. O. B. Rygg, 'Nonlinear refraction–diffraction of surface waves in intermediate and shallow water', *Coastal Eng.*, **12,** 191–211 (1988).
16. K. H. Wang, T. Y. Wu and G. T. Yates, 'Scattering and diffraction of solitary waves by a vertical cylinder', *Preprints 17th Symp. on Naval Hydrodynamics, Sessions 7 and 8*, 1988, pp. 37–46, National Academy Press, Washington, D.C., 1989.
17. D. H. Peregrine, 'Equations for water waves and the approximation behind them', in R. E. Meyer (ed.), *Waves on Beaches*, Academic Press, New York, 1972, pp. 357–412.
18. T. Y. Wu, 'Long waves in ocean and coastal waters', *Proc. ASCE, J. Eng. Mech. Div.*, **107,** (EM3), 501–522 (1981).
19. G. Pedersen, 'On the numerical solution of the Boussinesq equations', *University of Oslo, Research Report in Mechanics 88-14*, 1988.
20. G. Pedersen and O. B. Rygg, 'Numerical solution of the three dimensional Boussinesq equations for dispersive surface waves', *University of Oslo, Research Report in Mechanics 88-1*, 1987.
21. G. B. Whitham, 'Linear and nonlinear waves', in *Pure Appl. Math.*, Wiley, 1974.
22. H. Lamb, *Hydrodynamics*, Cambridge University Press, 1975.
23. M. S. Longuet-Higgins and J. D. Fenton, 'On the mass, momentum, energy and circulation of a solitary wave. II', *Proc. R. Soc. Lond. Ser. A*, **340,** 471–493 (1974).
24. J. Witting, 'On the highest and other solitary waves', *SIAM J. Appl. Math.*, **28,** 700–719 (1975).
25. J. W. Miles, 'Solitary waves', *Ann. Rev. Fluid Mech.*, **12,** 11–43 (1980).
26. J. W. Miles, 'Diffraction of solitary waves', *Z. Angew. Math. Phys.*, **28,** 889–902 (1977).
27. A. G. Kulikovskii and V. A. Reutov, 'Movement of solitary and periodic waves with an amplitude close to the limiting in a liquid layer of slowly varying depth', *Fluid Dyn.*, **11,** 884–893 (1976).
28. A. G. Kulikovskii and V. A. Reutov, 'Propagation of nonlinear waves above semi-infinite underwater troughs and ridges', *Fluid Dyn.*, **15,** 217–224 (1980).
29. R. Grimshaw, 'The solitary wave in water of variable depth', *J. Fluid. Mech.*, **42,** 639–656 (1970).
30. M. Funakoshi, 'Reflection of obliquely incident solitary waves', *J. Phys. Soc. Jpn.*, **49,** 2371–2379 (1980).
31. F. Mesinger and A. Arakawa, 'Numerical methods used in atmospheric models', *GARP, Publ. Ser. WMO, Vol. 17*, 1976.
32. L. W. Schwartz and J. D. Fenton, 'Strongly nonlinear waves', *Ann. Rev. Fluid Mech.*, **14,** 39–60 (1982).